Taylor & Francis
Taylor & Francis Group

Fatigue crack growth simulations of bi-material interfacial cracks under thermo-elastic loading by extended finite element method

Himanshu Pathak[a], Akhilendra Singh[a]* and Indra Vir Singh[b]

[a]Department of Mechanical Engineering, IIT Patna, Patna, India; [b]Department of Mechanical and Industrial Engineering, IIT Roorkee, Roorkee, India

In this paper, fatigue crack growth simulations of bi-material interfacial cracks have been performed using extended finite element method (XFEM) under thermo-elastic loading. The material discontinuity (interface) has been modelled by a signed distance function whereas a strong discontinuity (crack) has been modelled by two functions i.e. Heaviside and asymptotic crack tip enrichment functions. The values of stress intensity factors are extracted from the XFEM solution by domain based interaction integral approach. Standard Paris fatigue crack growth law is used for the life estimation of various model problems. The results obtained by XFEM for an interfacial edge and centre cracks are compared with those obtained by finite element method based on a remeshing approach.

Keywords: XFEM; Paris law; bi-material; interfacial crack; stress intensity factors

1. Introduction

Bi-materials are widely used in engineering structures/components, which are subjected to extreme loadings like mechanical, thermal and combinations of both. The residual stresses are generated in these components as a result of non-uniform thermal expansion of the two materials during heating and cooling. Bi-materials are designed with an aim to decrease the residual stresses, and to prevent debonding at the interface. The study of cracks under thermo-elastic loading is becoming increasingly important in the design of various machine components. The design against fatigue failure in these types of structures/components is associated with many challenges due to the complexity in accurately evaluating the fracture parameters at the interface. The evaluation of fracture parameters such as stress intensity factors (SIFs) becomes quite essential for the simulation based design. Only a limited number of studies have been reported in the literature on the interface fatigue crack growth even if the effect of the thermal loading on the bi-material was studied by several authors. Olsson and Giannakopoulos (1997) presented a combined analytical and numerical study to investigate the fracture parameters of plane stress edge cracks in bi-material beam structures. They also devised the closed form solution for an elasto-plastic material under thermal loading. Guru-murthy, Jiao, Norris, Hui, and Kramer (1998) have developed a new experimental technique that uses an optic displacement sensor to investigate the crack growth along polymer interfaces under thermal fatigue conditions. Johnson and Qu, (2006) extended the interaction integral approach so that the effect of non-uniform temperatures can be taken into account while

---

*Corresponding author. Email: akhil@iitp.ac.in

calculating the SIFs for cracks in a bi-material interface. Rakin, Kolednik, Medjo, Simha, and Fischer (2009) have carried out an experimental study on a bi-material compact tension specimen to see the effect of residual stress. Drai, Bouiadjra, Meddah, and Benguediab (2009) have used the finite element method (FEM) to analyse the behaviour of interface cracks at ceramic-metal interface under thermal residual stresses. They found that the mode II (the sliding mode) is the dominant mode of failure under thermal loading. Khandelwal and Kishen (2009) have proposed a method to compute the SIFs for a bi-material interface crack subjected to thermal loading. The proposed method is validated by solving the standard problems with known solutions. Boutabout et al. (2009) have used finite element models to simulate the mixed mode crack propagation near the bi-material interface under combined thermo mechanical loading. Petrova and Schmauder (2011) theoretically analysed the thermal interface crack problem in a bi-material with internal defects. They derived the thermal SIFs as a function of geometry.

To assess the fracture parameters and fatigue life of the materials, experiments need to be conducted on specimens with a pre-existing crack. Due to the difficulties and expense associated with conducting such experiments, considerable efforts have been made to simulate the cracks using numerical methods. The methods such as FEMs, boundary element methods (Yan, 2006; Yan & Nguyen Dang, 1995), meshfree methods (Belytschko, Gu, & Lu, 1994; Belytschko, Lu, & Gu, 1995; Duflot & Nguyen Dang, 2004) are available to solve fracture problems. Over the years, a number of approaches have been developed in FEM, which makes it a most suitable method for analysing fracture problems. In finite element analyses, the geometry is modelled by an adequate mesh. However, the generation of conforming meshes is an expensive task for complex geometries. In FEM, a crack must coincide with edges of finite elements i.e. a conformal mesh is required as well as special elements to handle crack tip asymptotic stress fields. FEM often experiences difficulties in remeshing and adaptive analysis. Hence, the modelling and simulation of discontinuities and defects using FEM becomes quite cumbersome. To overcome these difficulties, a novel approach known as the extended finite element method (XFEM) (Belytschko & Black, 1999; Melenk & Babuska, 1996) has been developed to handle discontinuous domain problems with ease. In XFEM, the standard displacement based approximation is enriched by additional functions using the partition of unity (Melenk & Babuska, 1996). The enrichment functions are added in the displacement approximation using the partition of unity. XFEM does not require a conformal mesh for crack growth modelling. The level set method (Stolarska, Chopp, Moës, & Belytschko, 2001; Sukumar, Chopp, Moës, & Belytschko, 2001; Ventura, Xu, & Belytschko, 2002) is combined with XFEM to model the crack growth. It has been widely used to solve problems of crack growth such as cohesive crack propagation (Asferg, Poulsen, & Nielson, 2007; Unger, Eckardt, & Konke, 2007; Zi & Belytschko, 2003), fatigue crack propagation (Chopp & Sukumar, 2003; Giner, Sukumar, Denia, & Fuenmayor, 2008; Stolarska & Chopp, 2003), three-dimensional crack propagation (Sukumar, Moës, Moran, & Belytschko, 2000) and fatigue life of homogenous plate (Singh, Mishra, Bhattacharya, & Patil, 2011) under mechanical loading.

In all above mentioned studies, the simulation of fatigue crack growth and fatigue life was limited to homogenous materials under mechanical loading. Therefore, the main aim of this study is to accurately evaluate the fatigue life of bi-material interfacial cracks under thermo-elastic loading. The fatigue crack growth is modelled with various small size line segments. The SIFs of bi-material interface cracks are numerically evaluated using the modified domain form of interaction integral approach. Generalised Paris' law is used to compute the fatigue life. A comparison of XFEM results with those obtained by FEM (remeshing approach using ANSYS 12.0) is presented for a few model problems.

2. Review of XFEM

XFEM is a modified form of the partition of unity finite element method (PUFEM) (Melenk & Babuska, 1996) and the generalised finite element method (GFEM) (Strouboulis, Babuska, & Copps, 2000; Strouboulis, Copps, & Babuska, 2000). PUFEM is based on a global enrichment technique while GFEM uses different shape functions for classical and enriched approximation. In contrast to PUFEM and GFEM, where the enrichments are usually employed over the entire domain, XFEM adopts the same procedure on a local level. According to the nature of the problem, the partition of unity enrichment is applied on the selected nodes to capture required physical phenomena. The formulation of XFEM is similar to the FEM. In general, it uses Langrage interpolation functions to approximate the field variables as well as the geometry. In FEM formulation, the field variable u is approximated by a Lagrange interpolation $u(\mathbf{x})$ (Möes, Dolbow, & Belytschko, 1999), which is given as:

$$u(x) = p^T(x)\, a = \sum_{j=1}^{n} N_j u_j \tag{1}$$

where $p(x)$ is the complete basis vector, a is a set of unknown coefficient and N_j are the shape functions.

In XFEM, the primary variables for a crack problem are approximated by Lagrange interpolation functions as defined in Equation (1) along with additional enrichment terms (Möes et al., 1999):

$$u(x) = \sum_{j=1}^{n} N_j(x) \left[u_j + \underbrace{[H(x) - H(x_I)]a_j}_{j\,\varepsilon\,n_s} + \underbrace{\chi(x)b_j}_{j\,\varepsilon\,n_r} + \underbrace{\sum_{\alpha=1}^{4} [\beta_\alpha(x) - \beta_\alpha(x_I)]c_j^\alpha}_{j\,\varepsilon\,n_t} \right] \tag{2}$$

where N_j are the Lagrange shape functions, u_j is the field variable for the continuous part of the XFEM solution, a_j is the additional degree of freedom associated with Heaviside function $H(x)$ used for the crack face, b_j is the additional degrees of freedom (DOF) associated with signed distance function χ used for simulating material discontinuity and c_j^α are additional DOFs associated with the four asymptotic enrichment functions used for the crack tip singularity. n is the set of all nodes associated with the element, n_s is the set of all nodes associated with the crack face, n_r is the set of nodes which belongs to the weak discontinuity and n_t is the set of nodes associated with the crack tip. The additional degrees of freedom associated with the enriched nodes correspond to either strong or weak discontinuity. No element can have both discontinuities altogether at a particular node. Initially, an element is searched for both types of discontinuities, and if a particular element belongs to the strong (crack) as well as the weak (interface) then preference is given to the strong discontinuity. Since, the elements having crack as well as material interface create the spurious singular modes in the linear system of equations therefore only strong enrichment was recommended (Sukumar, Huang, Prevost, & Suo, 2004) for these elements. Hence, the set of nodes n_r and n_t remains always disjointed.

3. Problem formulation

A domain Ω is separated into two different materials as shown in Figure 1. The equilibrium and boundary conditions for a linear thermo-elastic problem with small displacement bounded by Γ may be described as
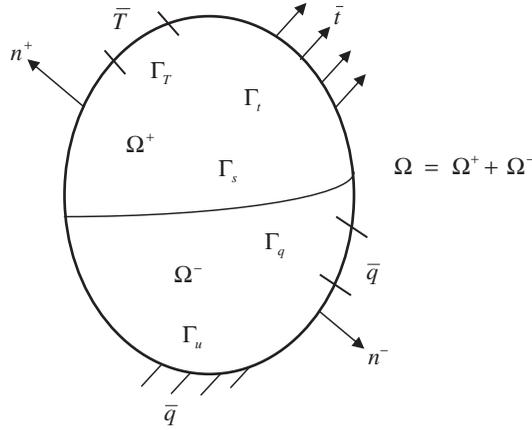
Figure 1.   2D inhomogeneous body.

$$-\nabla q + Q = 0 \text{ where } q = -k\nabla T \tag{3}$$

$$\nabla.\sigma + b = 0 \text{ where } \sigma = C:(\varepsilon - \varepsilon_T) \tag{4}$$

and thermo-elastic strain tensor may be defined as $\varepsilon = \nabla_s u$ and $\varepsilon_T = \alpha(T - T_{ref})I \tag{5}$

The boundary conditions for the problem domain can be defined as

$$T = \bar{T} \text{ on } \Gamma_T \text{ and } q \, . \, n = \bar{q} \text{ on } \Gamma_q \tag{6a}$$

$$\sigma.n = \bar{t} \text{ on } \Gamma_t \text{ and } u = \bar{u} \text{ on } \Gamma_u \tag{6b}$$

In the above governing equations, q is the heat flux vector, Q represents the heat source, k is the thermal conductivity of materials, σ is the Cauchy stress tensor, b is the body force vector, $\nabla.$ is the divergence operator, C is the isotropic fourth order tensor, ∇_s is the symmetric gradient operator, u shows the displacement vector, T is the temperature field within the domain, ε_T is the thermal strain vector with respect to reference temperature T_{ref}, α is the thermal expansion coefficient and I represents the second order identity tensor. The above boundary conditions satisfy $\Gamma_T \cup \Gamma_q = \Gamma_u \cup \Gamma_t = \Gamma$ and $\Gamma_T \cap \Gamma_q = \Gamma_u \cap \Gamma_t = \Phi$, $\Gamma_c \subset \Gamma_t$, $\bar{t} = 0$ on Γ_c for the crack surface. In case of thermo-elastic adiabatic crack $\Gamma_c \subset \Gamma_q$, $\bar{q} = 0$ on Γ_c whereas in case of thermo-elastic isothermal crack $\Gamma_c \subset \Gamma_T$, $\bar{T} = \bar{T}_c$ on Γ_c.

3.1.   *Mechanical loading*

In case of mechanical loading, the weak form of governing Equation (4) can be written as (Möes et al., 1999):

$$\int_\Omega \boldsymbol{\sigma}:\varepsilon(\mathbf{v})d\Omega - \int_\Omega \mathbf{b}.\mathbf{v}d\Omega - \int_{\Gamma_t} \bar{\mathbf{t}}.\mathbf{v}\,d\Gamma = 0 \quad \forall \mathbf{v} \in u_o \tag{7}$$

where the test function space is $u_o = \{v \in \Re : v = 0 \text{ on } \Gamma_{\text{c}}, \ v \text{ possibly discontinuous on } \Gamma_{\text{c}}\}$ (8)

Introducing the constitutive equation in the weak form, Equation (7) becomes:

$$\int_{\Omega} \varepsilon(\mathbf{u}) : C : \varepsilon(v) \, d\Omega - \int_{\Omega} b.v \, d\Omega - \int_{\Gamma_t} \bar{t}.v \, d\Gamma = 0 \quad \forall v \in u_o \tag{9}$$

The above equation is equivalent to the strong form (4) of the governing equation, which includes the traction free boundary condition at the crack surface. The discrete equations are obtained by introducing displacement approximations, weight and shape functions in Equation (9).

3.2. Thermo-elastic loading

In a thermo-elastic adiabatic crack problem, both temperature and displacement fields are discontinuous across the crack surface whereas heat flux is singular at the crack tip (Sih, 1962). Therefore, displacement and temperature fields may be defined as:

$$u_o = \{u \in \Re : u = \bar{u} \text{ on } \Gamma_{\text{u}}, \ u \text{ possibly discontinuous on } \Gamma_{\text{c}}\} \tag{10}$$

$$T_o = \{T \in \Re : T = \bar{T} \text{ on } \Gamma_{\text{T}}, \ T \text{ possibly discontinuous on } \Gamma_{\text{c}}\} \tag{11}$$

In case of a thermo-elastic isothermal crack domain, a specific temperature is prescribed at the crack surface; hence essential boundary conditions are imposed at the crack surface. In contrast with an adiabatic crack, the following salient features have been found for an isothermal crack (Duflot, 2008):

- the heat flux is discontinuous across the crack surface;
- the temperature field is continuous across the crack surface; and
- the angular variation of temperature and flux field is different from an adiabatic crack. In case of an adiabatic crack, they vary in direction of perpendicular to the crack surface, whereas in case of an isothermal crack, they vary in radial direction.

The temperature field may be defined as

$$T_o = \{T \in \Re : T = \bar{T} \text{ on } \Gamma_{\text{T}} / \Gamma_{\text{c}}, \ q \text{ possibly discontinuous on } \Gamma_{\text{c}}\} \tag{12}$$

The weak form of governing Equation (3) using constitutive equation becomes (Möes, Cloirec, Cartraud, & Remacle, 2003):

$$\int_{\Omega} q(S) \, k \, q(T) \, d\Omega + \int_{\Omega} S \, Q \, d\Omega - \int_{\Gamma_q} S \, \bar{q} d\Gamma = 0 \tag{13}$$

$$\int_{\Omega} \varepsilon(\mathbf{u}) : C : \varepsilon(v) d\Omega - \int_{\Omega} b.v \, d\Omega - \int_{\Gamma_t} \bar{t}.v \, d\Gamma - \int_{\Omega} \varepsilon_T(\mathbf{u}) : C : \varepsilon(v) \, d\Omega = 0 \tag{14}$$

In case of an isothermal crack, the essential boundary conditions are applied on the crack surface. Hence, the weak form is modified accordingly.

After introducing the displacement approximation, trial and test functions, and using the arbitrariness of nodal variation, a set of discrete equations can be written as:

$$[K]\{u\} = \{f\} \tag{15}$$

where u is the vector of field variables, K and f are the XFEM global stiffness matrix and external force vector, respectively. The stiffness matrix and force vector are computed on an element level and are assembled into their global position through usual assembly procedure. Higher order Gauss quadrature (seventh order quadrature in each sub-elements of tip element and second order quadrature in each sub-element of split and interface elements) has been used in discontinuous elements. The additional DOFs arise due to enrichment using the fictitious nodes. The element contribution of K and f are as follows

$$K_{ij}^e = \begin{bmatrix} K_{ij}^{uu} & K_{ij}^{ua} & K_{ij}^{ub} & K_{ij}^{uc} \\ K_{ij}^{au} & K_{ij}^{aa} & K_{ij}^{ab} & K_{ij}^{ac} \\ K_{ij}^{bu} & K_{ij}^{ba} & K_{ij}^{bb} & K_{ij}^{bc} \\ K_{ij}^{cu} & K_{ij}^{ca} & K_{ij}^{cb} & K_{ij}^{cc} \end{bmatrix} \tag{16a}$$

$$f^e = \{f_i^u \quad f_i^a \quad f_i^b \quad f_i^{c1} \quad f_i^{c2} \quad f_i^{c3} \quad f_i^{c4}\}^T \tag{16b}$$

$$K_{ij}^{rs} = \int_{\Omega^e} (B_i^r)^T D B_j^s \, d\Omega, \text{ where } r, s = u, a, b, c \tag{16c}$$

$$f_i^u = \int_{\Gamma_t} N_i \bar{t} \, d\Gamma + \int_{\Omega_e} N_i b \, d\Omega \tag{16d}$$

$$f_i^a = \int_{\Gamma_t} N_i [H(x) - H(x_I)] \bar{t} \, d\Gamma + \int_{\Omega_e} N_i [H(x) - H(x_I)] b \, d\Omega \tag{16e}$$

$$f_i^b = \int_{\Gamma_t} N_i \chi(x) \, \bar{t} \, d\Gamma + \int_{\Omega_e} N_i \chi(x) \, b \, d\Omega \tag{16f}$$

$$f_i^{c\alpha} = \int_{\Gamma_t} N_i [\beta_\alpha(x) - \beta_\alpha(x_I)] \, \bar{t} \, d\Gamma + \int_{\Omega_e} N_i [\beta_\alpha(x) - \beta_\alpha(x_I)] \, b \, d\Omega, \text{ where } \alpha = 1, 2, 3, 4 \tag{16g}$$

$$B_i^u = \begin{bmatrix} N_{i,x} & 0 \\ 0 & N_{i,y} \\ N_{i,y} & N_{i,x} \end{bmatrix} \tag{16h}$$

$$B_i^a = \begin{bmatrix} (N_i[H(x) - H(x_I)])_{,x} & 0 \\ 0 & (N_i[H(x) - H(x_I)])_{,y} \\ (N_i[H(x) - H(x_I)])_{,y} & (N_i[H(x) - H(x_I)])_{,x} \end{bmatrix} \tag{16i}$$

$$B_i^b = \begin{bmatrix} (N_i\chi(x))_{,x} & 0 \\ 0 & (N_i\chi(x))_{,y} \\ (N_i\chi(x))_{,y} & (N_i\chi(x))_{,x} \end{bmatrix} \tag{16j}$$

$$B_i^{c\alpha} = \begin{bmatrix} (N_i[\beta_\alpha(x) - \beta_\alpha(x_I)])_{,x} & 0 \\ 0 & (N_i[\beta_\alpha(x) - \beta_\alpha(x_I)])_{,y} \\ (N_i[\beta_\alpha(x) - \beta_\alpha(x_I)])_{,y} & (N_i[\beta_\alpha(x) - \beta_\alpha(x_I)])_{,x} \end{bmatrix}, \quad \text{where } \alpha = 1, 2, 3, 4 \tag{16k}$$

$$\mathbf{D} = \frac{E}{1 - v^2} \begin{bmatrix} 1 & v & 0 \\ v & 1 & 0 \\ 0 & 0 & \frac{1-v}{2} \end{bmatrix} \text{ for plane stress} \tag{16l}$$

3.3. Enrichment functions

Heaviside function, used for the modelling of discontinuities in displacement and temperature fields can be defined as (Mohammadi et al., 2008):

$$H(x) = \begin{cases} 1 & \text{if}(x - x^*).n \geqslant 0 \\ -1 & \text{otherwise} \end{cases} \tag{17}$$

Level set approach (Sukumar et al., 2001) is used to capture the weak discontinuity, which arises due to the material interface within the element. An enrichment function for the material interface is defined as

$$\chi(x) = \sum_I N_I |\zeta_I| - \left| \sum_I N_I \zeta_I \right| \tag{18}$$

where $\zeta(\Phi(x)) = |\Phi(x)|$ is the signed distance function, and Φ is the level set function, which is defined as:

$$\Phi(x) = \pm\min\|x - x_\Gamma\| \tag{19}$$

In this work, a signed distance function along with four crack tip enrichment functions are used to capture the stress singularity at the crack tip in bi-material domains. This allows the effective representation of the crack tip fields (Pant, Singh, & Mishra, 2011; Pathak, Singh, & Singh, 2012). The last enrichment term in Equation (2) consists of four functions obtained from the displacement solution of a linear elastic fracture problem (Anderson, 1995), and is defined as:

$$\beta_\alpha(x) = \left[\sqrt{r}\sin\frac{\theta}{2}, \sqrt{r}\cos\frac{\theta}{2}, \sqrt{r}\cos\frac{\theta}{2}\sin\theta, \sqrt{r}\sin\frac{\theta}{2}\sin\theta \right] \tag{20}$$

3.4. Interaction integral for mechanical and thermo-elastic loading

The domain based interaction energy integral method is a very efficient technique to extract the individual SIFs (K_I, K_{II}) under mixed mode loading conditions. For a bi-material interface crack, the *J*-integral remains globally path independent if material homogeneity exists in the direction parallel to the crack surface under both mechanical and thermo-elastic loading (Johnson & Qu, 2006). The standard path independent *J*-integral for a crack domain can be defined as

$$J = \int_\Gamma \left[W_s\delta_{1j} - \sigma_{ij}\frac{\partial u_i}{\partial x_1} \right] n_j d\Gamma \tag{21}$$

where Γ is an arbitrary contour which encloses the crack tip, W_s is the strain energy density, n_j is the outward unit normal to the contour and δ_{1j} is the Kronecker delta function. The coordinate value has been taken as the local coordinate parallel to crack surface. Two independent equilibrium states have been taken to evaluate interaction integrals; state 1 corresponds to an actual state while state 2 is taken as auxiliary state, obtained from analytical solutions of asymptotic stress and displacement fields. After introducing actual and auxiliary fields, the *J*-integral can be defined as

$$J^{(1+2)} = J^{(1)} + J^{(2)} + M^{(1,2)} \tag{22}$$

Here, $J^{(1+2)}$ is the *J*-integral of the superimposed state, $J^{(1)}$ is the *J*-integral in the actual state, $J^{(2)}$ is the *J*-integral due to the auxiliary state and $M^{(1,2)}$ is the interaction term.

The domain form of the interaction integral under mechanical loading can be written as

$$M^{(1,2)} = \int_A \left[\sigma_{ij}^{(1)}\frac{\partial u_i^{(2)}}{\partial x_1} + \sigma_{ij}^{(2)}\frac{\partial u_i^{(1)}}{\partial x_1} - W^{(1,2)}\delta_{ij} \right] \frac{\partial q}{\partial x_j} dA \tag{23}$$

$$W^{(1,2)} = \frac{1}{2}(\sigma_{ij}^{(1)}\varepsilon_{ij}^{(2)} + \sigma_{ij}^{(2)}\varepsilon_{ij}^{(1)}) \tag{24}$$

where q is a scalar weight function where the value is one at the crack tip and zero at the contour. $\sigma_{ij}^{(1)}$ and $\varepsilon_{ij}^{(1)}$, are the actual Cauchy stress and engineering strain, respectively, while $\sigma_{ij}^{(2)}$ and $\varepsilon_{ij}^{(2)}$ are the auxiliary Cauchy stress and engineering strain, respectively. $W^{(1,2)}$ represents the strain energy density at actual and auxiliary states. Similarly, the thermal interaction integral proposed by (Sills & Dolev, 2004) as:

$$M^{(1,2)} = \int_A \left[\sigma_{ij}^{(1)}\frac{\partial u_i^{(2)}}{\partial x_1} + \sigma_{ij}^{(2)}\frac{\partial u_i^{(1)}}{\partial x_1} - W^{(1,2)}\delta_{ij} \right] \frac{\partial q}{\partial x_j} dA + \alpha \int_A \frac{\partial T}{\partial x_1}\sigma_{kk}^{(2)} q dA \tag{25}$$

For the bi-material crack domain, the interaction integral can be modified due to the presence of two different materials as:

$$M^{(1,2)} = \sum_{m=1}^{2} \int_{A_k} \left[\sigma_{ij}^{(1)} \frac{\partial u_i^{(2)}}{\partial x_1} + \sigma_{ij}^{(2)} \frac{\partial u_i^{(1)}}{\partial x_1} - W^{(1,2)} \delta_{ij} \right] \frac{\partial q}{\partial x_j} dA + \sum_{m=1}^{2} \alpha \int_{A_k} \frac{\partial T}{\partial x_1} \sigma_{kk}^{(2)} q dA \qquad (26)$$

where m represents a particular material in the bi-material domain. The auxiliary field equations for the bi-material domain are taken from (Sukumar et al., 2004).

For linear elastic problems, the interaction integral is related to the mixed mode SIFs by the following relation:

$$M^{(1,2)} = \frac{2}{H} (K_I^{(1)} K_I^{(2)} + K_{II}^{(1)} K_{II}^{(2)}) \qquad (27)$$

$$\text{where,} \frac{1}{H} = \frac{1/E_1 + 1/E_2}{2 \cosh^2 \pi \varepsilon} \qquad (28)$$

In Equation (27), $K_I^{(2)}$ and $K_{II}^{(2)}$ are the auxiliary field SIFs and ε is the bi-material constant defined as:

$$\varepsilon = \frac{1}{2\pi} \log \left(\frac{1 - \bar{\beta}}{1 + \bar{\beta}} \right) \qquad (29)$$

where β is the second Dundurs parameter given by,:

$$\bar{\beta} = \frac{\mu_1(\kappa_2 - 1) - \mu_2(\kappa_1 - 1)}{\mu_1(\kappa_2 + 1) + \mu_2(\kappa_1 + 1)} \qquad (30)$$

$$\kappa_i = \frac{3 - \upsilon_i}{1 + \upsilon_i} \quad \text{for plane stress} \qquad (31)$$

where μ_i, υ_i and κ_i are the shear modulus, Poisson's ratio and Kolosov constants for corresponding materials. The mixed mode SIFs can be calculated from Equation (27) using $K_I^{(2)}=1$, $K_{II}^{(2)}=0$ and vice versa.

3.5. Fatigue analysis

In the present work, fatigue crack growth simulations are performed under constant amplitude cyclic loading. The bi-material interfacial crack domain is subjected to two different types of cyclic loading, namely mechanical and thermo-elastic. For the cyclic mechanical loading problems, the discrete equations are solved for displacement fields then SIFs are evaluated using the modified form of the interaction integral method. In the thermo-elastic problems, thermal discrete equations are solved for temperature distribution. These results are used as a load input for the elastic discrete equations, which are further solved for the displacement field. In the post processing phase, thermal interaction integral in Equation (26) is used for evaluating the SIFs. The range of SIF for constant amplitude cyclic loading is defined as:

$$\Delta K = K_{\max} - K_{\min} \qquad (32)$$

where, K_{max} and K_{min} are the SIFs corresponding to maximum and minimum applied loads, respectively. In general, a crack path is curved in nature but it can be modelled accurately using many small straight crack segments. The crack growth direction has been obtained by using a maximum principal stress criterion which assumes that the crack may grow in a direction perpendicular to the maximum principal stress. Therefore, for each crack increment, a crack growth direction θ_c has been obtained as (Erdogan & Sih, 1963):

$$K_I \sin \theta_c + K_{II}(3 \cos \theta_c - 1) = 0 \tag{33}$$

After solving (33), we obtained:

$$\theta_c = 2 \tan^{-1} \left(\frac{K_I - \sqrt{K_I^2 + 8K_{II}^2}}{4K_{II}} \right) \tag{34}$$

Equation (34) gives two values of θ_c. One of these values corresponds to a maximum and the other one corresponds to a minimum. The value of θ_c corresponding to the maximum equivalent SIF may be used to find ΔK_{Ieq} using Equation (35) given below:

$$\Delta K_{Ieq} = \Delta K_I \cos^3 \left(\frac{\theta_c}{2} \right) - 3\Delta K_{II} \cos^2 \left(\frac{\theta_c}{2} \right) \sin \left(\frac{\theta_c}{2} \right) \tag{35}$$

In the present work, it is assumed that the interface toughness is relatively high; so a crack may kink into anyone of the bulk materials depending upon the loading, boundary condition and material properties (Hutchinson, 1992). Crack kinking behaviour has been studied for two dissimilar bulk materials without considering the effect of interface material. The kinking criterion presented by (Hutchinson, 1992) to select a particular bulk material is given as:

$$\frac{G_{kink}}{G_{int}} > \frac{(G_c)_{kink}}{(G_c)_{int}} \tag{36}$$

where, G_{kink} is the energy release rate at crack kinked position, G_{int} is the energy release rate for crack advance along its interface, $(G_c)_{kink}$ is the critical energy release rate of the bulk material in which the crack kinks in and $(G_c)_{int}$ is referred to as the interface toughness. In the present work, this kinking criterion has been modified in terms of SIFs, and is given below:

$$\text{Depending on } \theta_c \text{value} \left\{ \frac{(\Delta K_{Ieq})_{m1}}{(K_{IC})_{m1}} \text{ or } \frac{(\Delta K_{Ieq})_{m2}}{(K_{IC})_{m2}} \right\} > \frac{(\Delta K_{Ieq})_{int}}{(K_{IC})_{int}} \tag{37}$$

In the above equation, the values of θ_c and ΔK_{Ieq} obtained using Equations (34) and (35) belong to either material-1 (m1) or material-2 (m2). If Z1>Z2 then the crack propagates in either first or second material along 0=0c otherwise it propagates along the interface at 0=0. For the interface, the maximum ΔK_{Ieq} will be equal to ΔK_I corresponding to $\theta = 0$. To implement this modified criterion, two ratios Z_1 and Z_2 are calculated as:

$$Z_1 = \frac{(\Delta K_{Ieq})_{m1}}{(K_{IC})_{m1}} \text{ or } \frac{(\Delta K_{Ieq})_{m2}}{(K_{IC})_{m2}} \text{ depending on } \theta_c, Z_2 = \frac{(\Delta K_{Ieq})_{int}}{(K_{IC})_{int}} \tag{38}$$

where m_1 and m_2 signify material 1 and material 2 of the bi-layer. If $Z_1 > Z_2$ then the crack propagates in either first or second material along $\theta = \theta_c$ otherwise it propagates along the interface at $\theta = 0$.

For quasi-static crack propagation, (Paris, Gomez, & Anderson, 1961) have been proposed a mathematical mode to obtain fatigue life under cyclic loading:

$$\frac{da}{dN} = C(\Delta K_{Ieq})^m \tag{39}$$

where a is the crack length, N is the number of loading cycles, C and m are the material constant for the Paris model. After determining the magnitude and direction of the crack segment, the crack length, tip and split nodes get modified by the level sets. Two separate level sets have been used in this work to track and update a moving discontinuity. The first level set is used to track the crack while the second one is used for the bi-material interface. An optimal value of the crack segment needs to be taken for the simulation. If a crack segment is taken too small then it requires a very fine mesh near the crack tip so that the tip must fall in a new element at each step. A large size of crack increment would not represent the real crack path. Therefore, an increment of 2 mm (one tenth of the initial crack length) has been taken for the crack growth simulations.

4.   Results and discussion

The fatigue analyses of bi-material interfacial crack problems under cyclic mechanical and cyclic thermo-elastic loadings have been performed by XFEM. A generalised MATLAB code has been developed to obtain the results. Extrinsic enrichment technique has been used to capture the effect of discontinuities in the problem domain. To capture the effect of strong discontinuities in the domain, Heaviside and crack tip enrichment functions are used, whereas to model the effect of weak discontinuity, a signed distance enrichment function has been used. In case of thermo-elastic loading, the problem is decoupled into thermal problem and elastic problem. First, the temperature distribution is obtained for the entire domain by solving the thermal problem, then it used as input in the elastic problem. Finally, the displacement based discrete equations are solved for the displacement field variables. Lagrange multiplier approach has been used to impose the essential boundary conditions i.e. temperature. For numerical integration, two point Gauss quadrature has been used in those elements which do not have any discontinuity, while higher order Gauss quadrature along with sub-triangulation is used in discontinuous elements. The distribution of Gauss points for the entire domain is shown in Figure 2 whereas Figure 3 shows the Gauss point distribution for the crack tip element. Three different fatigue cases of bi-material interface cracks have been considered in this study. The results are presented in the form of number of life cycles and SIFs $(\text{MPa}\sqrt{m})$. For all cases, the crack faces are taken parallel to the material interface. The FEM results are obtained by ANSYS software using remeshing. A plane stress condition has been assumed in all the simulations.

4.1.   Mechanical loading

A bi-material rectangular plate of size $100\,\text{mm} \times 200\,\text{mm}$ containing an interfacial centre or an edge crack is considered for the simulation. The problem domain is discretized using four noded Lagrangian type quadrilateral elements. The uniformly distributed 30 nodes in x-direction and 60 nodes in y-direction i.e. total 1800 nodes have been created in the domain.
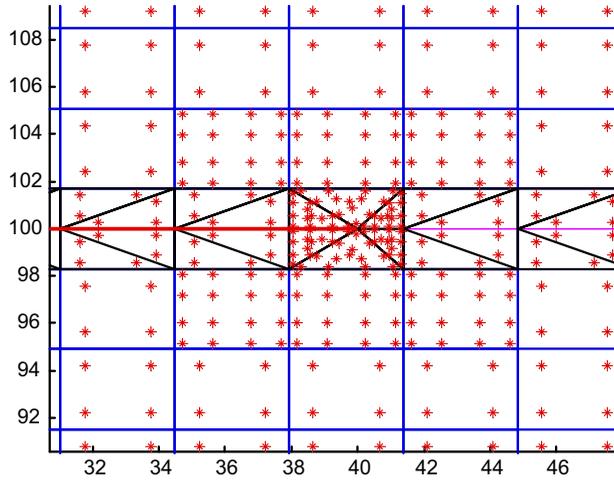
Figure 2.   Gauss point distribution and sub-triangulation for numerical integration.
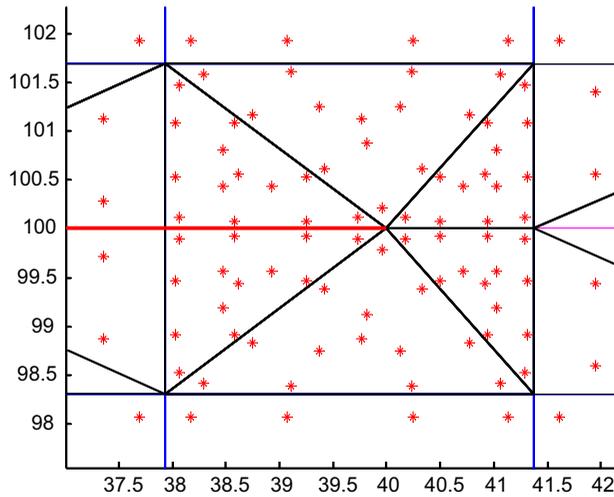
Figure 3.   Crack tip element sub-triangulation with Gauss point distribution for numerical integration.

The model problem contains an edge crack of length $a = 10$ mm and centre crack of length $2a = 20$ mm, and is solved under cyclic mechanical loading. The boundary conditions along with other parameters used in modelling of bi-material plates are shown in Figures 4 and 5. A cyclic load of $\sigma_{\min} = 0\,N/mm$ and $\sigma_{\max} = 100\,N/mm$ is applied at the top edge of the plate whereas the bottom edge is constrained in y-direction. The values of Poisson's ratio and Paris exponent for both materials of the plate are taken as $v = .3$ and $m = 3$, respectively. The other material properties such as Young's moduli, fracture toughness and Paris constant for both materials of the plate are taken as $E_1 = 74$ GPa, $E_2 = 200$ GPa, $K_{IC1} = 40 MPa\sqrt{m}$, $K_{IC2} = 60 MPa\sqrt{m}$, $C_1 = 2.087136 \times 10^{-11}$ and $C_2 = 2.087136 \times 10^{-12}$, respectively. The quasi-static crack propagation and fatigue life of plate are calculated with XFEM and FEM (remeshing approach). The value of the crack increment is taken as 2 mm at each step of the crack growth. This problem is also solved with FEM using a remeshing approach where
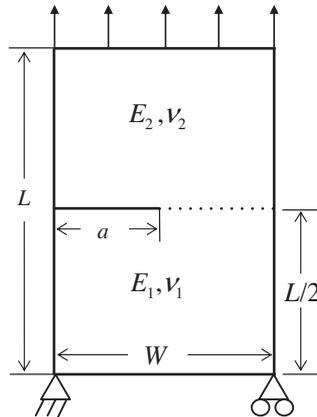
Figure 4. Physical domain of bi-material edge crack under cyclic mechanical loading.
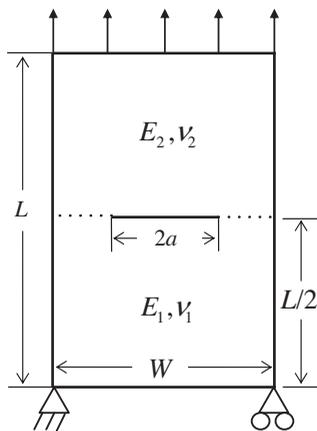
Figure 5. Physical domain of bi-material centre crack under cyclic mechanical loading.

fatigue crack propagation is simulated in steps. In case of the centre crack problem, the values of the SIFs at both tips are found to be similar, therefore an equal crack increment is taken at both of the crack tips. The SIFs at each step of the crack growth are then used to evaluate fatigue life using Paris law. The SIFs and fatigue life obtained with XFEM and FEM for an edge crack and centre crack problems are presented in Figures 6–9. Figure 6 presents the plot of SIFs with crack extension for an edge crack problem whereas Figure 7 shows the fatigue life with crack extension for an edge crack problem. The star marked in the figure indicates the final fatigue life of the plate. The fatigue life and critical crack extension obtained with XFEM are found as *5484* cycles and *14.51* mm, respectively, whereas the fatigue life and critical crack extension obtained with remeshing approach are found as *5406* cycles and *14.99* mm, respectively. Figures 8 and 9 show the SIFs and fatigue life for a bi-material centre crack problem. These plots show that the fatigue failure life and corresponding crack extension obtained with XFEM are *16,649* cycles and *40.81* mm whereas the fatigue life and crack extension obtained with the remeshing approach are found as *16,327* cycles and 41.36 mm, respectively. From the results presented in these figures, it is clear that the
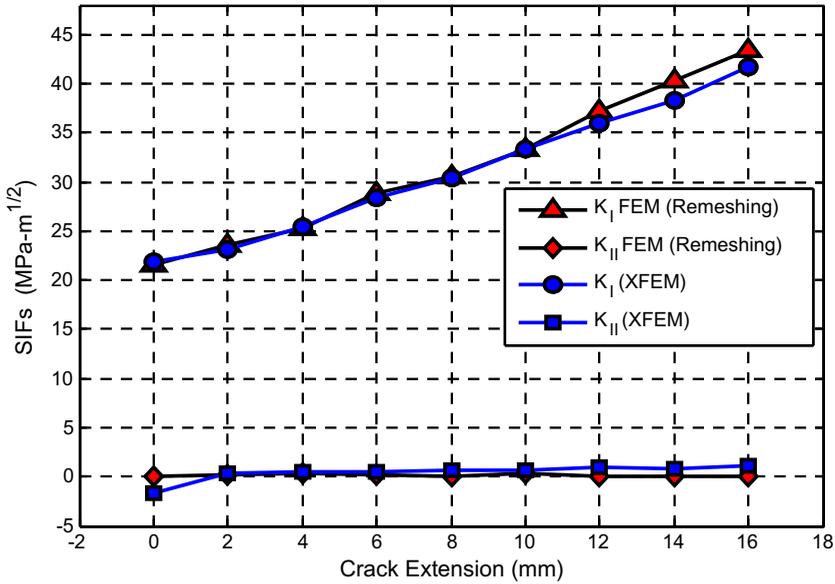
Figure 6.   SIFs for a bi-material edge crack under cyclic mechanical loading.
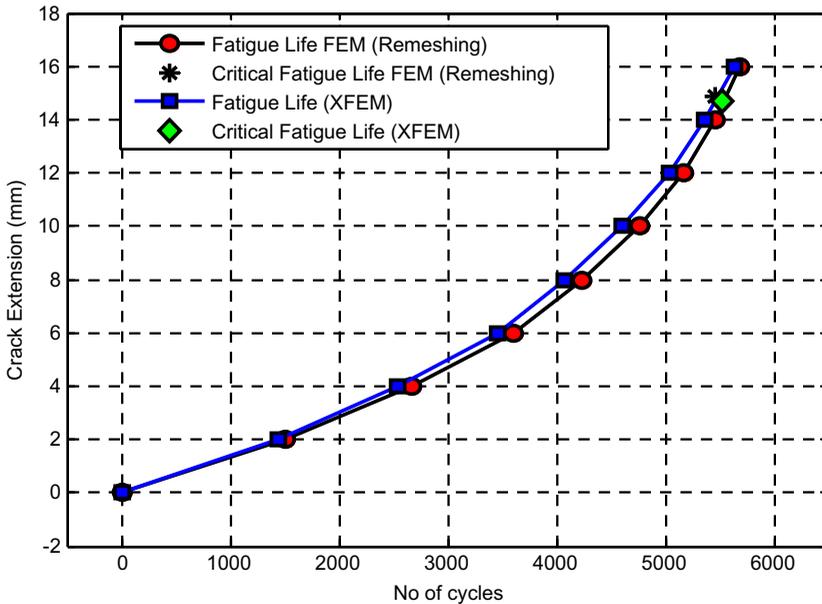
Figure 7.   Fatigue-life for a bi-material edge crack under cyclic mechanical loading.

fatigue life of an edge cracked plate is reduced to *67.06*% compared to the one of the same length centre cracked plate under an equivalent mechanical loading. The fatigue life of an edge crack is found to be 67.06% less as compared to the same length centre crack problem under the same mechanical load. From the cracked domain, it is found that the crack kinks out of the interface towards the soft material. From these results, it is also observed that the results obtained from XFEM are quite close to the one of the remeshing approach (ANSYS).
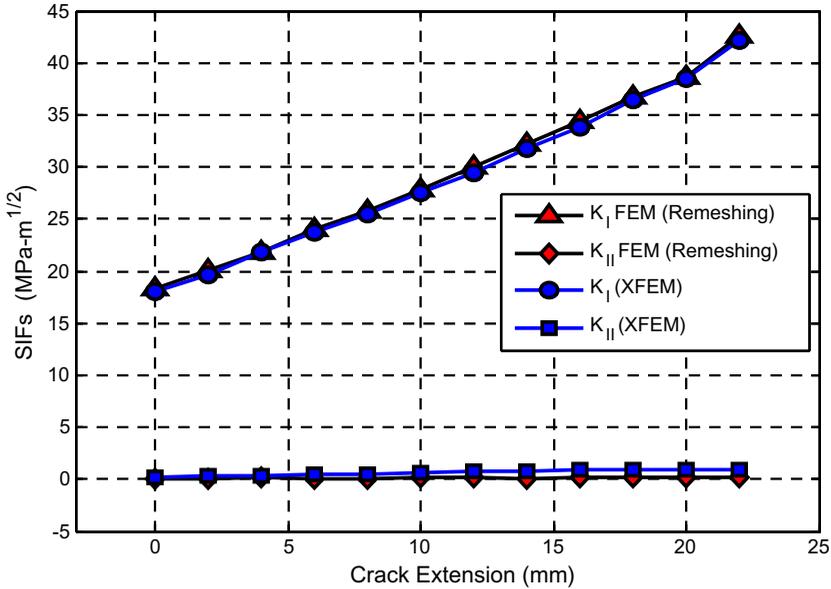
Figure 8.   SIFs for a bi-material centre crack under cyclic mechanical loading.
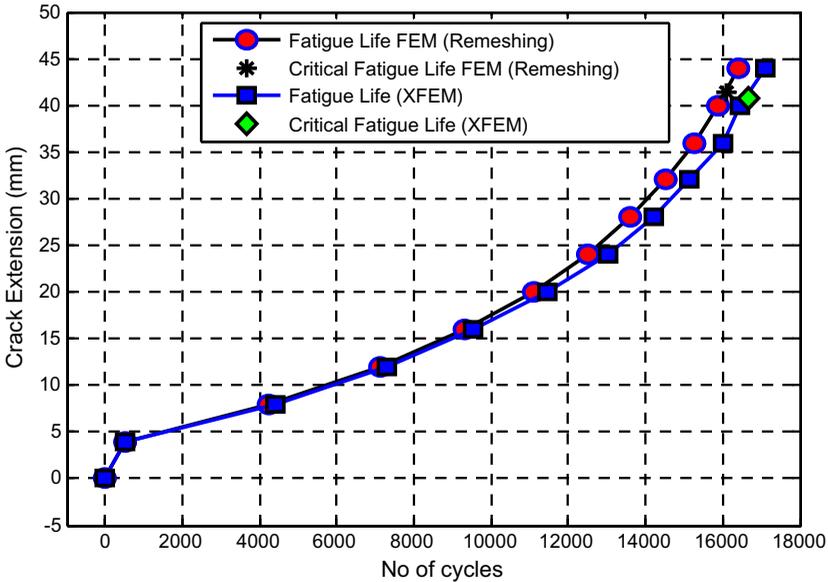
Figure 9.   Fatigue-life for a bi-material centre crack under cyclic mechanical loading.

4.2.   *Thermo-elastic loading*

The thermo-elastic problems are solved by decoupling them into thermal and structural problems. First, heat equations are solved for temperature distribution within the domain; then this temperature data is used as boundary conditions to solve elastic equations. The thermal interaction integral approach is implemented to extract mixed mode SIFs. According to the type

of thermal boundary conditions used in the model problems, thermo-elastic problems are sub-divided into two groups: adiabatic crack and isothermal crack.

4.2.1. *Adiabatic crack*

For an adiabatic crack, both displacement and temperature fields are discontinuous across the crack surface, and heat flux becomes singular at the crack tip. Heaviside function has been used to capture discontinuity in temperature as well as in displacement fields; whereas four crack tip functions are used to model singularity in heat flux and stress fields. The approximation of temperature and displacement fields can be written as

$$T(x) = \sum_{j=1}^{n} N_j(x) \left[T_j + \underbrace{[H(x) - H(x_I)]a_j}_{j \, \varepsilon \, n_s} + \underbrace{\chi(x)b_j}_{j \, \varepsilon \, n_r} + \underbrace{\sum_{\alpha=1}^{4} [\beta_\alpha(x) - \beta_\alpha(x_I)]c_j^\alpha}_{j \, \varepsilon \, n_t} \right] \tag{40}$$

$$u(x) = \sum_{j=1}^{n} N_j(x) \left[u_j + \underbrace{[H(x) - H(x_I)]a_j}_{j \, \varepsilon \, n_s} + \underbrace{\chi(x)b_j}_{j \, \varepsilon \, n_r} + \underbrace{\sum_{\alpha=1}^{4} [\beta_\alpha(x) - \beta_\alpha(x_I)]c_j^\alpha}_{j \, \varepsilon \, n_t} \right] \tag{41}$$

A bi-material plate of size $100 \, \text{mm} \times 200 \, \text{mm}$ containing an interfacial centre or an edge crack is considered for the simulations. The interfacial edge and centre cracks of length $a = 10 \, \text{mm}$ and $2a = 20 \, \text{mm}$, respectively, are solved under cyclic thermal loading. The boundary conditions along with other parameters are shown in Figures 10 and 11 for an edge and centre crack, respectively. In case of cyclic thermal loading, $T_1 = -200 \, ^\circ\text{C}$ and $T_2 = 200 \, ^\circ\text{C}$ are imposed on the plates for maximum thermal load whereas for minimum thermal load T_1 and T_2 becomes zero. A constant heat flux is applied across the crack surface. The uniformly distributed 30 nodes in x-direction and 60 nodes in y-directions i.e. total 1800 nodes have been
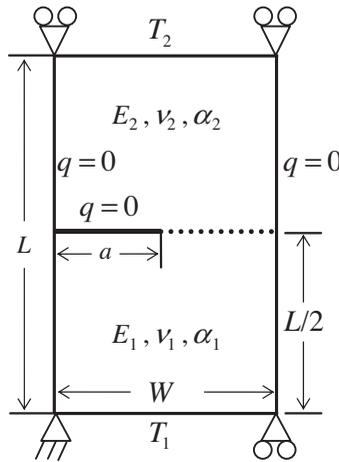
Figure 10.   Physical domain of bi-material adiabatic edge crack with cyclic heat flux.
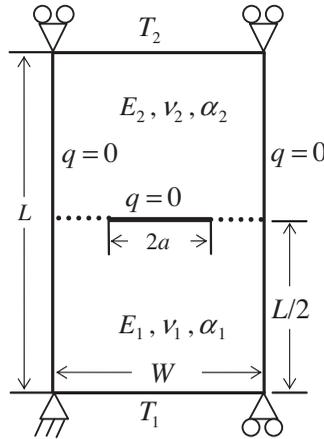
Figure 11.   Physical domain of bi-material adiabatic centre crack with cyclic heat flux.
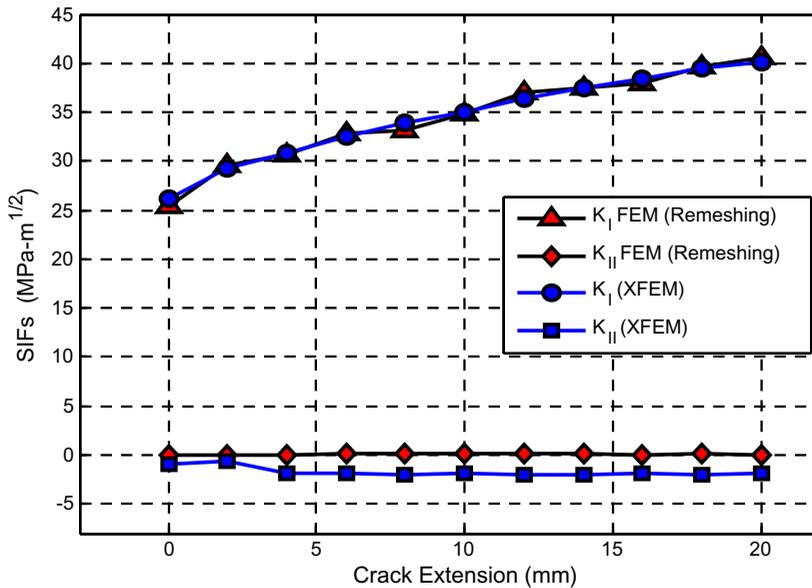
Figure 12.   SIFs for a bi-material adiabatic edge crack under cyclic heat flux.

created within the rectangular domain of the plate. The thermal material properties such as thermal conductivity and thermal expansion coefficient are taken as $K_{th1} = 250$ W/mK, $K_{th2} = 50$ W/mK, $\alpha_1 = 20 \times 10^{-6}/°$C and $\alpha_1 = 15 \times 10^{-6}/°$C in all the simulations. A crack increment of 2 mm (one tenth of the initial crack length) is taken at each crack tip. The quasi-static crack growth and fatigue life of plates are obtained from XFEM and FEM using remeshing approaches. The results obtained with XFEM and remeshing approaches are presented in Figures 12 and 13 for an edge crack problem. From these figures, the fatigue life and corresponding crack extension obtained with XFEM are found to be *4120* cycles and *18.82* mm, whereas the fatigue life and crack extension obtained with the remeshing approach are found to be *4229* cycles and *18.71* mm, respectively. Figures 14 and 15 present the SIFs and fatigue
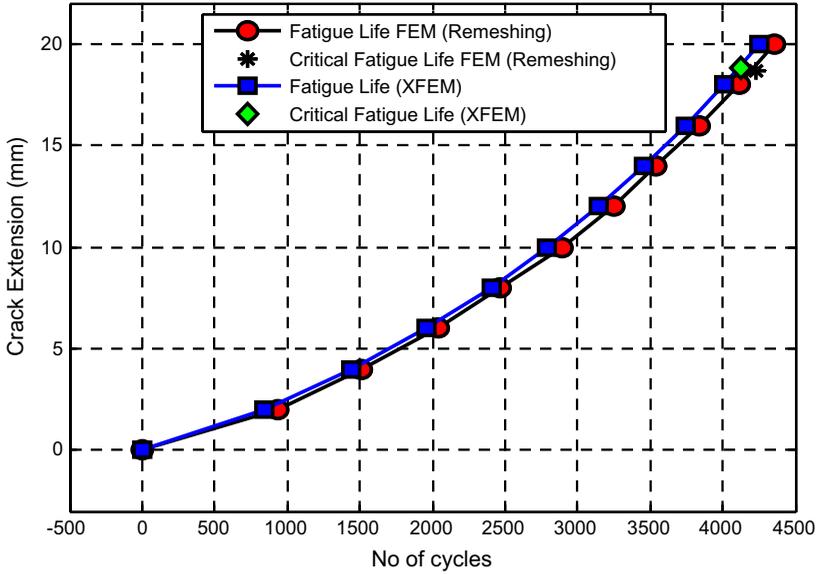
Figure 13. Fatigue-life for a bi-material adiabatic edge crack under cyclic heat flux.

life obtained with XFEM and remeshing for a centre crack problem. The fatigue failure life and corresponding crack extension obtained with XFEM are found to be *3571* cycles and *36.45* mm, respectively, whereas the fatigue life and corresponding crack extension obtained with the remeshing approach are found to be *3430* cycles and 37.02 mm. The crack path trajectory for an adiabatic edge crack has been presented in Figure 16(a) and (b) whereas the trajectory for an adiabatic centre crack has been shown in Figures 17(a) and (b). The magnified
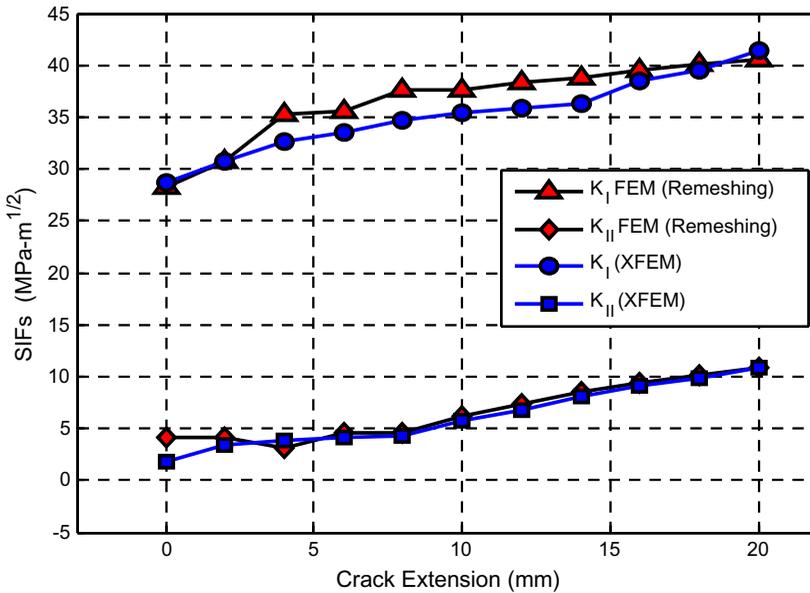
Figure 14. SIFs for a bi-material adiabatic centre crack under cyclic heat flux.
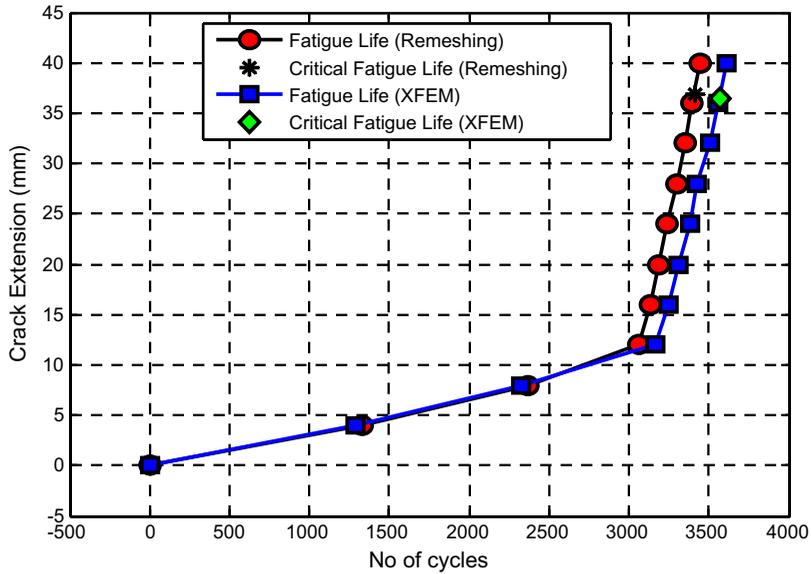
Figure 15. Fatigue-life for a bi-material adiabatic centre crack under cyclic heat flux.
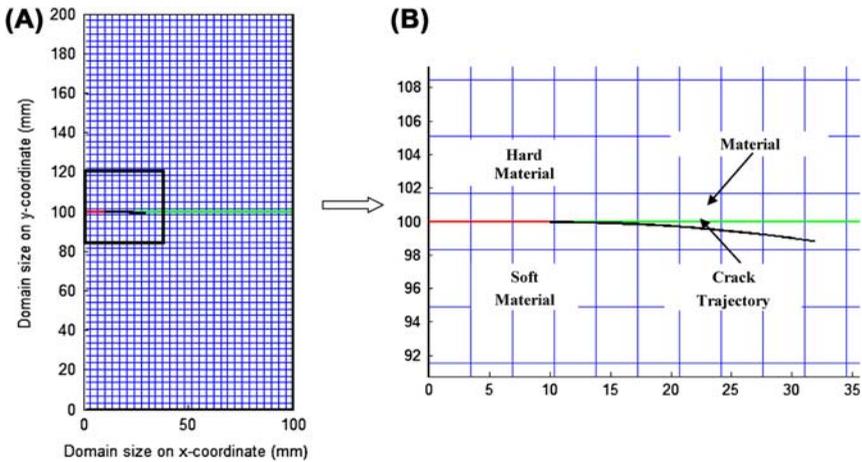
Figure 16. (a) Adiabatic edge crack domain with final crack trajectory. (b) Magnified view of crack trajectory.

views of crack trajectory show that the crack kinks towards the soft material. On the basis of these simulations it is observed that the reduction in the fatigue life of the edge cracked plate is quite significant as compared to the same length centre crack plate for thermo-elastic loading. It is also seen that the results obtained with XFEM and remeshing approaches are quite close to each other.

4.2.2. *Isothermal crack*

In case of an isothermal crack, the essential boundary condition i.e. temperature is prescribed at the crack surface $T = \bar{T}$ on Γ_c. In FEM, the essential boundary conditions can be easily
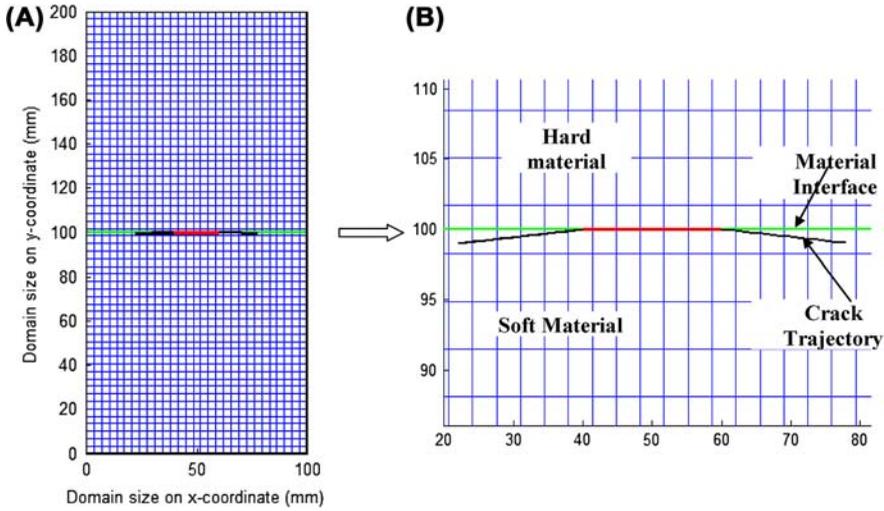
Figure 17.   (a) Adiabatic centre crack domain with final crack trajectory. (b) Magnified view of crack trajectory.

imposed using the Lagrange multiplier approach as the crack faces coincides with element edges, whereas in XFEM, the crack faces do not coincide with element edges, thereby the imposition of temperature at the crack faces becomes more burdensome. Due to the difficulties associated with imposing essential boundary condition in non-conformal meshed domain; various approaches have been developed by Möes, Béchet, and Tourbier (2006), Géniaut, Massin, and Moës (2007), and Béchet, Moës, and Wohlmuth (2009) to solve this issue. In the present work, an approximate approach based on the Lagrange multiplier is used to impose the essential boundary conditions. First, the elements intersected by the crack are identified using the level set approach, and then the temperature is directly prescribed at the nodes of these elements using the Lagrange multiplier approach. Since these nodes are aligned with the mesh interface (exactly not lying at crack surface), the EBC can be easily
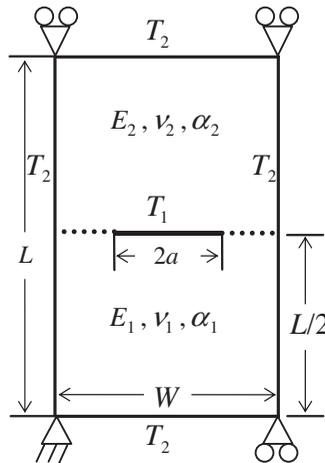
Figure 18.   Physical domain of bi-material isothermal centre crack with cyclic heat flux.
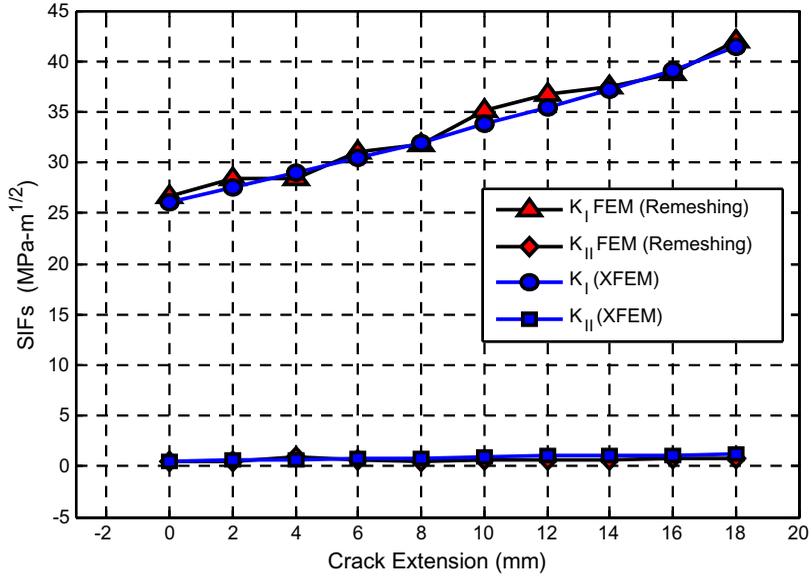
Figure 19. SIFs for a bi-material isothermal centre crack under cyclic heat flux.
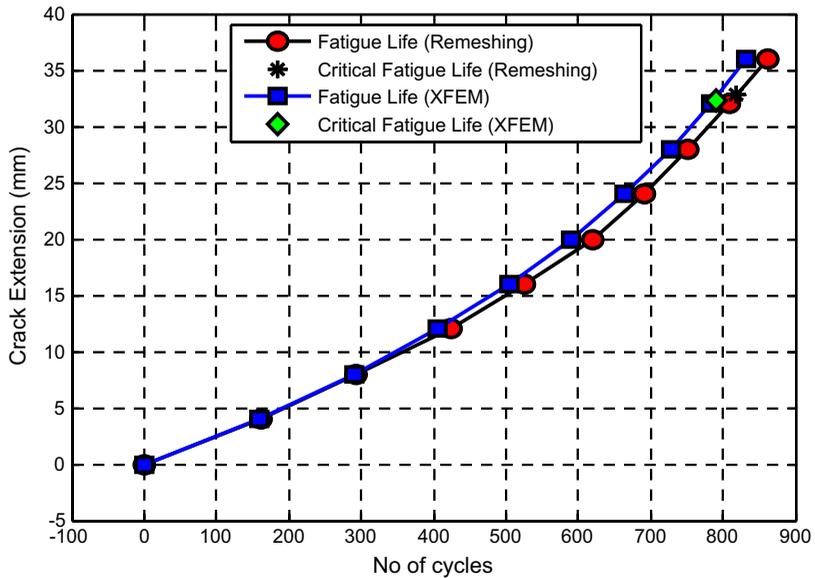
Figure 20. Fatigue life for a bi-material isothermal centre crack under cyclic heat flux.

implemented using the Lagrange multiplier approach. Moreover, these elements have been subdivided into triangular sub-elements to accurately perform the numerical integration. Thus, the conventional approach of interpolation based Lagrange multiplier efficiently take care of essential boundary condition (EBC) without compromising on the accuracy of the solution. To demonstrate the accuracy of this approach, temperature contours are provided in Figures
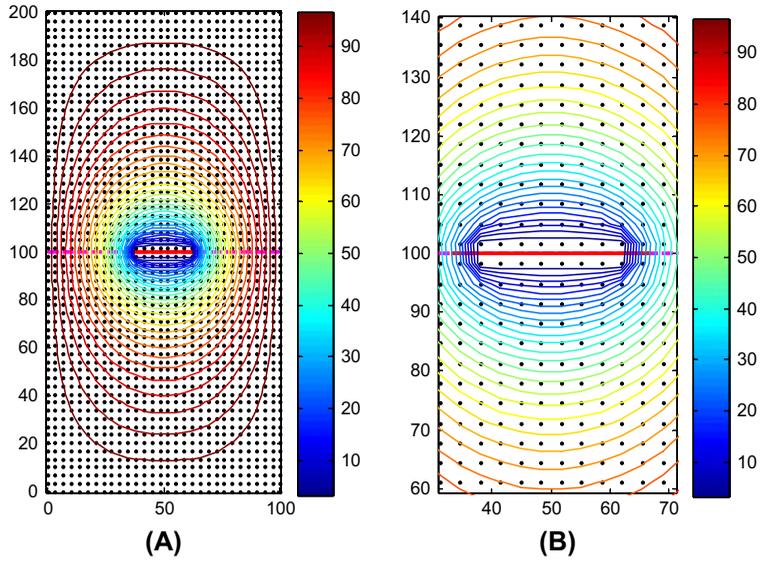
Figure 21. (a) Temperature contour at 30×60 nodes. (b) Magnified view of temperature contour at 30×60 nodes.
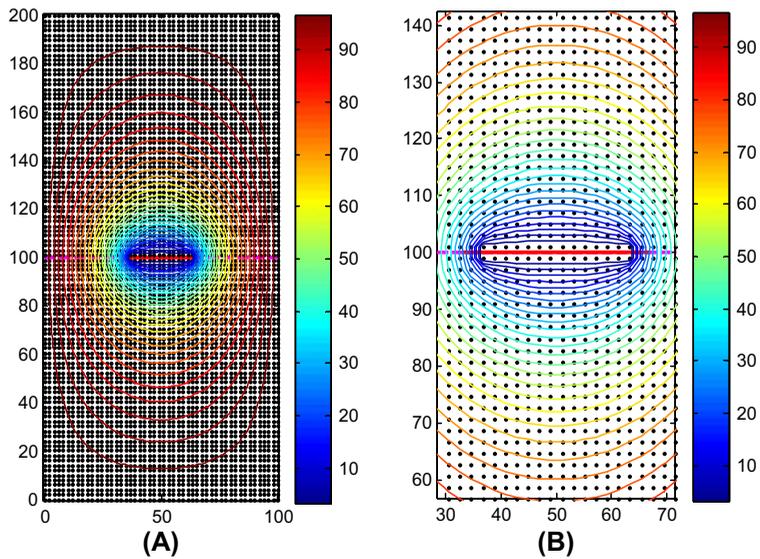
Figure 22. (a) Temperature contour at 50×100 nodes. (b) Magnified view of temperature contour at 50×100 nodes.

21–24, respectively, for four different sets of nodal data (30×60, 50×100, 70×140 and 90×180).

The leading terms of temperature and heat flux near an isothermal crack are as follows (Duflot, 2008):
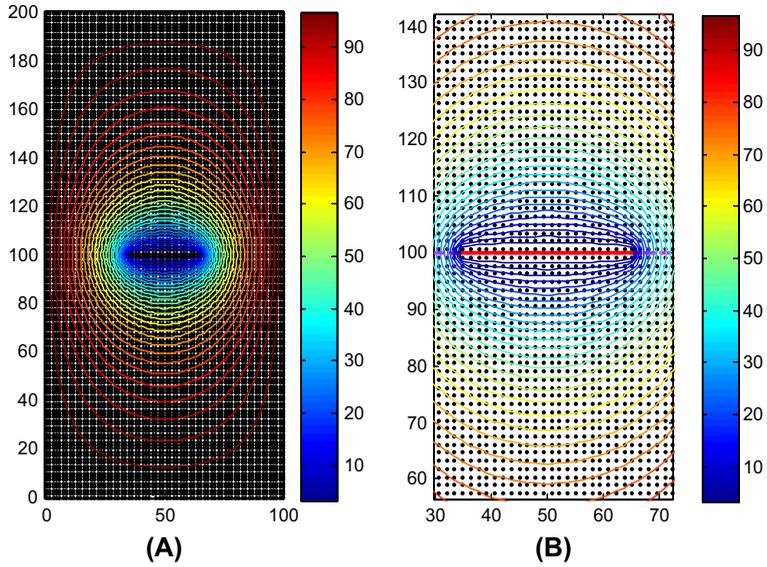
Figure 23. (a) Temperature contour at 70×140 nodes. (b) Magnified view of temperature contour at 70×140 nodes.
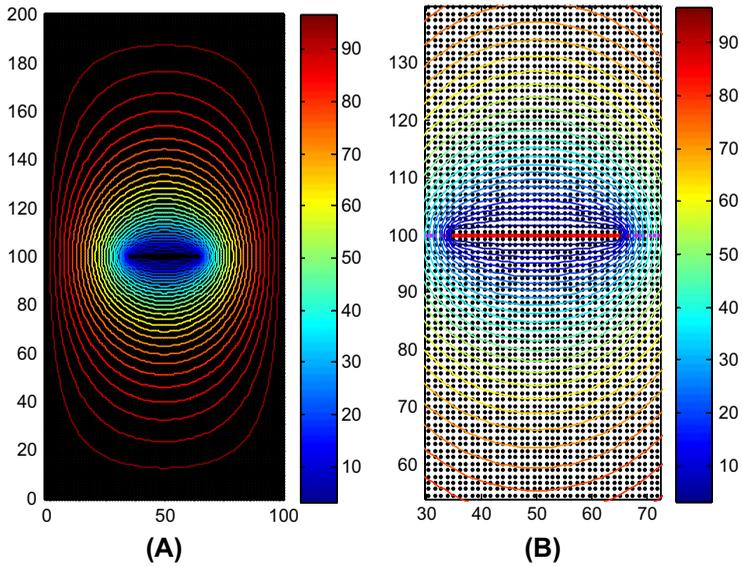
Figure 24. (a) Temperature contour at 90×180 nodes. (b) Magnified view of temperature contour at 90×180 nodes.

$$T = -\frac{K_T}{k} \sqrt{\frac{2r}{\pi}} \cos\left(\frac{\theta}{2}\right) \qquad (42)$$

$$\mathbf{q} = \frac{K_T}{\sqrt{2\pi\, r}}(\cos(\tfrac{\theta}{2}) \atop \sin(\tfrac{\theta}{2})) \tag{43}$$

The approximation of the temperature field and displacement field may be written as:

$$T(x) = \sum_{j=1}^{n} N_j(x) \left[T_j + \underbrace{\sqrt{r}\cos\frac{\theta}{2}c_j}_{j\,\varepsilon\,n_t} \right] \tag{44}$$

$$u(x) = \sum_{j=1}^{n} N_j(x) \left[u_j + \underbrace{[H(x) - H(x_I)]a_j}_{j\,\varepsilon\,n_s} + \underbrace{\chi(x)b_j}_{j\,\varepsilon\,n_r} + \underbrace{\sum_{\alpha=1}^{4} [\beta_\alpha(x) - \beta_\alpha(x_I)]c_j^\alpha}_{j\,\varepsilon\,n_t} \right] \tag{45}$$

A bi-material plate of size $100\,\text{mm} \times 200\,\text{mm}$ containing an interfacial centre crack of length $2a = 30\,\text{mm}$ has been simulated under cyclic thermal loading. The boundary conditions along with other parameters are shown in Figure 18. A constant amplitude cyclic thermal load has been applied over the domain. For maximum heat flux, the outer edge is exposed to $T_2 = 100\,°\text{C}$, while $T_1 = 0\,°\text{C}$ is maintained at the crack surface. Uniformly distributed 50 nodes in x-direction and 100 nodes in y-directions i.e. total 5000 nodes have been created in the rectangular plate. The quasi-static crack growth and fatigue life of the plate are obtained with XFEM and remeshing (ANSYS) approaches. The increment at each crack tip is taken as $2\,\text{mm}$. The SIF values and fatigue life obtained with XFEM and the remeshing approach are presented in Figures 19 and 20, respectively. The fatigue life obtained with XFEM is found to be *791* cycles with a corresponding crack extension of $32.26\,\text{mm}$ whereas the fatigue life and crack extension obtained with the remeshing approach are found to be *819* cycles and *32.89* mm, respectively. From the results presented in these figures, it is seen that these obtained with XFEM are found quite close to those obtained with a remeshing approach.

5. Conclusions

In the present work, bi-material interfacial crack problems are studied and analysed with XFEM under mechanical and thermo-elastic loadings. The fatigue life of bi-material crack plates is evaluated by generalised Paris law under mechanical and thermo-elastic loadings. XFEM based on extrinsic partition of unity enrichment has been successfully used to model both material and geometric discontinuities. The maximum principal stress criterion has been implemented to obtain crack growth direction. A generalised MATLAB code has been developed to obtain the results for various quasi-static crack growth problems. Various bi-material crack problems have been solved under mechanical as well as thermo-elastic loading. These simulations show that the fatigue life of an edge crack plate is found to be quite small as compared to the centre crack plate under similar loading and boundary conditions. In case of thermo-elastic loading, fatigue life of an isothermal crack has less fatigue life as compared to an adiabatic crack for similar loading conditions. The results obtained with extrinsic PU enriched XFEM were found to be in agreement with those obtained with the remeshing approach. During simulations, it was also noticed that XFEM can be easily and accurately

used to simulate both strong and weak discontinuities. Therefore, this work can be extended further to simulate complex quasi-static and stable crack growth problems.

Acknowledgements

References

Anderson T. L. (1995). *Fracture mechanics fundamentals and applications*. Boca Raton, FL: CRC Press, ISBN 0-8493-4260-0, 1995.

Asferg, J. L., Poulsen, P. N., & Nielsen, L. O. (2007). A consistent partly cracked XFEM element for cohesive crack growth. *International Journal for Numerical Methods in Engineering, 72*, 464–485.

Béchet, E., Moës, N., & Wohlmuth, B. (2009). A stable Lagrange multiplier space for stiff interface condition within the extended finite element method. *International Journal for Numerical Methods in Engineering, 78*, 931–954.

Belytschko, T., & Black, T. (1999). Elastic crack growth in finite elements with minimal remeshing. *International Journal for Numerical Methods in Engineering, 45*, 601–620.

Belytschko, T., Gu, L., & Lu, Y. Y. (1994). Fracture and crack growth by element-free Galerkin methods. *Modelling Simulation Material Science Engineering, 2*, 519–534.

Belytschko, T., Lu, Y. Y., & Gu, L. (1995). Crack propagation by element-free Galerkin methods. *Engineering Fracture Mechanics, 51*, 295–315.

Boutabout, B., Chama, M., Abbes, B., Bouiadjra, B., Serier, B., & Lousdad, A. (2009). Effect of thermo mechanical loads on the propagation of crack near the interface brittle/ductile. *Computational Materials Science, 46*, 906–911.

Chopp, D. L., & Sukumar, N. (2003). Fatigue crack propagation of multiple coplanar cracks with the coupled extended finite element/fast marching method. *International Journal of Engineering Science, 41*, 845–869.

Drai, A., Bouiadjra, B. B., Meddah, M., & Benguediab, M. (2009). Analysis of interfacial fracture in ceramic–metal assemblies under effect of thermal residual stresses. *Computational Materials Science, 46*, 1119–1123.

Duflot, M. (2008). The extended finite element method in thermo-elastic fracture mechanics. *International Journal for Numerical Methods in Engineering, 74*, 827–847.

Duflot, M., & Nguyen-Dang, H. (2004). A meshless method with enriched weight functions for fatigue crack growth. *International Journal for Numerical Methods in Engineering, 59*, 1945–1961.

Erdogan, F., & Sih, G. (1963). On the crack extension in plates under plane loading and transverse shear. *Journal of Basic Engineering, 85*, 519–527.

Géniaut, S., Massin, P., & Moës, N. (2007). A stable 3D contact formulation using X-FEM. *European Journal of Computational Mechanics, 16*(2), 259–275.

Giner, E., Sukumar, N., Denia, F. D., & Fuenmayor, F. J. (2008). Extended finite element method for fretting fatigue crack propagation. *International Journal of Solids and Structure, 45*, 5675–5687.

Gurumurthy, C. K., Jiao, J., Norris, L. G., Hui, C. Y., & Kramer, E. J. (1998). A thermo-mechanical approach for fatigue testing of polymer bimaterial interfaces. *Journal of Electronic Packaging, 120*, 372–378.

Hutchinson, J. W. (1992). Mixed mode cracking in layered materials. *Advances in Applied Mechanics, 29*, 63–191.

Johnson, J., & Qu, J. (2006). An interaction integral method for computing mixed mode stress intensity factors for curved bimaterial interface cracks in non-uniform temperature fields. *Engineering Fracture Mechanics, 74*, 2282–2291.

Khandelwal, R., & Kishen, J. M. C. (2009). Computation of thermal stress intensity factors for bimaterial interface cracks using domain integral method. *Journal of Applied Mechanics, 76*, 041010–41019.

Melenk, J., & Babuska, I. (1996). The partition of unity finite element method: Basic theory and applications. *Computer Methods in Applied Mechanics in Engineering, 139*, 289–314.

Moës, N., Béchet, E., & Tourbier, M. (2006). Imposing Dirichlet boundary conditions in the extended finite element method. *International Journal for Numerical Methods in Engineering, 67*, 1641–1669.

Moës, N., Cloirec, M., Cartraud, P., & Remacle, J. F. (2003). A computational approach to handle complex microstructure geometries. *Computer Methods in Applied Mechanics and Engineering, 192*, 3163–3177.

Moës, N., Dolbow, J., & Belytschko, T. (1999). A finite element method for crack growth without remeshing. *International Journal for Numerical Methods in Engineering, 46*, 135–150.

Mohammadi, S. (2008). *Extended finite element method for fracture analysis of structures*. Singapore: Blackwell, ISBN-978-1-4051-7060-4.

Olsson, M., & Giannakopoulos, A. E. (1997). Elastoplastic analysis of layered materials under thermal loading: Edge cracks parallel to the interface. *International Journal of Fracture, 85*, 81–97.

Pant, M., Singh, I. V., & Mishra, B. K. (2011). Evaluation of mixed mode stress intensity factors for interface cracks using EFGM. *Applied Mathematical Modeling, 35*, 3443–3459.

Paris, P. C., Gomez, M. P., & Anderson, W. E. (1961). A rational analytic theory of fatigue. *The Trend in Engineering, 13*, 9–14.

Pathak, H., Singh, A., & Singh, I. V. (2012). Numerical simulation of bi-material interfacial cracks using EFGM and XFEM. *International Journal of Mechanics and Materials in Design, 8*, 9–36.

Petrova, V., & Schmauder, S. (2011). Thermal fracture of a functionally graded/homogeneous bimaterial with system of cracks. *Theoretical and Applied Fracture Mechanics, 55*, 148–157.

Rakin, M., Kolednik, O., Medjo, B., Simha, N. K., & Fischer, F. D. (2009). A case study on the effect of thermal residual stresses on the crack-driving force in linear-elastic bimaterials. *International Journal of Mechanical Sciences, 51*(7), 531–540.

Sih, G. C. (1962). On singular character of thermal stress near a crack tip. *Journal of Applied Mechanics, 51*, 587–598.

Sills, L. B., & Dolev, O. (2004). The conservative M-integral for thermo-elastic problems. *International Journal of Fracture, 125*, 149–170.

Singh, I. V., Mishra, B. K., Bhattacharya, S., & Patil, R. U. (2011). The numerical simulation of fatigue crack growth using extended finite element method. *International Journal of Fatigue, 36*, 109–119.

Stolarska, M., & Chopp, D. L. (2003). Modeling thermal fatigue cracking in integrated circuits by level sets and the extended finite element method. *International Journal of Engineering Science, 41*, 2381–2410.

Stolarska, M., Chopp, D. L., Moës, N., & Belytschko, T. (2001). Modeling crack growth by level sets in the extended finite element method. *International Journal for Numerical Methods in Engineering, 51*, 943–960.

Strouboulis, T., Babuska, I., & Copps, K. (2000). The design and analysis of the generalized finite element method. *Computer Methods in Applied Mechanics and Engineering, 181*, 43–69.

Strouboulis, T., Copps, K., & Babuska, I. (2000). The generalized finite element method: An example of its implementation and illustration of its performance. *International Journal of Numerical Methods in Engineering, 47*, 1401–1417.

Sukumar, N., Chopp, D. L., Moës, N., & Belytschko, T. (2001). Modeling holes and inclusions by level sets in the extended finite element method. *Computer Methods in Applied Mechanics in Engineering, 190*, 6183–6200.

Sukumar, N., Huang, Z. Y., Prevost, J. H., & Suo, Z. (2004). Partition of unity enrichment for bimaterial interface cracks. *International Journal for Numerical Methods in Engineering, 59*, 1075–1102.

Sukumar, N., Moës, N., Moran, B., & Belytschko, T. (2000). Extended finite element method for three-dimensional crack modeling. *International Journal for Numerical Methods in Engineering, 48*, 1549–1570.

Unger, J. F., Eckardt, S., & Könke, C. (2007). Modelling of cohesive crack growth in concrete structures with the extended finite element method. *Computer Methods in Applied Mechanics in Engineering, 196*, 4087–4100.

Ventura, G., Xu, J. X., & Belytschko, T. (2002). A vector level set method and new discontinuity approximations for crack growth by EFG. *International Journal for Numerical Methods in Engineering, 54*, 923–944.

Yan, A. M., & Nguyen Dang, H. (1995). Multiple-cracked fatigue crack growth by BEM. *Computational Mechanics, 16*, 273–280.

Yan, X. (2006). A boundary element modeling of fatigue crack growth in a plane elastic plate. *Mechanics Research Communications, 33*, 470–481.

Zi, G., & Belytschko, T. (2003). New crack-tip elements for XFEM and applications to cohesive cracks. *International Journal for Numerical Methods in Engineering, 57*, 2221–2240.